

Silver Nanoparticles With Antimicrobial Activities Against Streptococcus Mutans And Their Cytotoxic Effect- Review Article

Dr. Vijay sir¹, Karthiga.N²

1. *Reader, Dept. of Pediatric Dentistry, Sree Balaji Dental College and Hospital., Bharath Institute of Higher Education and Research, Chennai*
2. *Undergraduate Student, Sree Balaji Dental College and Hospital, Bharath Institute of Higher Education and Research, Chennai.*

Corresponding Author Dr. Vijay sir

Reader, Dept. of Pediatric Dentistry, Sree Balaji Dental College and Hospital., Bharath Institute of Higher Education and Research, Chennai.

Phone no: 98844-11172

Abstract;

Microbial resistance represents a challenge for the scientific community to develop new bioactive compounds. The goal of this research was to evaluate the antimicrobial activity of silver nanoparticles (AgNPs) against a clinical isolate of Streptococcus mutans, antibiofilm activity against mature S. mutans biofilms and the compatibility with human fibroblasts. The antimicrobial activity of AgNPs against the planktonic clinical isolate was size and concentration dependent, with smaller AgNPs having a lower minimum inhibitory concentration. A reduction of 2.3 log in the number of colony-forming units of S. mutans was observed when biofilms grown in a CDC reactor were exposed to 100 ppm of AgNPs of 9.5 ± 1.1 nm. However, AgNPs at high concentrations (N10 ppm) showed a cytotoxic effect upon human dermal fibroblasts. AgNPs effectively inhibited the growth of a planktonic S. mutans clinical isolate and killed established S. mutans biofilms, which suggests that AgNPs could be used for prevention and treatment of dental caries. Further research and development are necessary to translate this technology into therapeutic and preventive strategies.

Keywords: inhibitory concentration, mutans, therapeutic, fibroblasts

INTRODUCTION

Biofilms are microbial consortia embedded in self-produced exopoly-mer matrices composed mainly of exopolysaccharides (EPS). Microbes living in these matrices benefit from nutrient and water supplies, improved lateral gene transfer and protection against adverse environmental insults, such as desiccation and chemicals, including detergents, disinfectants, and antibiotics[1]. Biofilms can be also reservoirs for pathogenic organisms and sources of disease outbreaks. For instance, biofilms are implicated in otitis media, otolaryngologic infections, osteomyelitis, bacterial endocarditis, cystic fibrosis, non-healing wounds and oral biofilm.

Dental caries and periodontal diseases are widespread diseases, both of which are highly prevalent in industrialized societies, and are rising in developing countries. Dental caries and periodontal diseases result from a complex interaction of environmental triggers, the resident microorganisms and the host. If the composition of an individual's resident oral microorganisms is out of balance, dental disease can occur. Even at the earliest times of initial colonization, flowing saliva bathes both cleaned surfaces and already attached cells with a variety of species suspended in saliva. A highly selective mechanism of coaggregation between species is involved in the development of multi-species communities. The primary initial colonizers are streptococci and some Actinomyces, and early colonizing veillonellae coaggregate with streptococci and

Actinomyces. Although culture independent sequencing has illuminated the complexity of the human oral microbiome, *Streptococcus mutans* remains widely regarded as a primary etiological agent in caries. This facultative anaerobic, Gram positive, bacterium excels in the complex environment of the oral cavity where stresses including low pH and an oxidative environment are coupled to variable salivary flow and carbohydrate supply. The physiologic adaptations of *S. mutans* to these pressures provide a competitive advantage versus non-cariogenic commensals that underpin the establishment and progression of caries.

Treatment of an infection after the biofilm is established is frequently futile with current remedies. Often, the only solution is the physical removal of the biofilm or implant, which is costly and traumatic to the patient. The control of oral biofilms depends in part on the use of chemical actives that kill or remove plaque. Actives that kill microorganisms presumably reduce bacterial virulence and retard the rate of plaque accumulation. The penetration of such actives into the microbial biofilm is a fundamental requirement for their efficacy. [2]

In recent years the application of nanoparticles in various fields has been expanded considerably. Nanoparticles have been successfully used in medical and pharmaceutical nano engineering for the delivery of therapeutic agents, in chronic disease diagnostics, and in sensors. AgNPs are efficient non-specific antimicrobial agents against planktonic forms of a broad spectrum of bacterial and fungal species. Their antimicrobial activities are attributed to the unique physicochemical characteristics of AgNPs, such as the high ratio of surface area to mass, high reactivity, and nanometer sizes, which confer them to a major advantage for the development of alternative products against multi-drug resistant microorganisms. Knowledge of nanoparticle diffusivity is a parameter necessary to understand the mobility, aggregation, and toxicity of these composites. The diffusion of nanoparticles may be hindered by: (i) the porous structure of the biofilm; (ii) the local accumulation of nanoparticles by cells, non-diffusing macromolecules, or the polysaccharide matrix; and (iii) the adsorption of the solute to freely diffusing species, abiotic particles, or gas bubbles. Due to the protection offered by the biofilm matrix to the diffusion of antibiotic agents within the copolymer matrix, the antimicrobial activity of AgNPs was tested against both planktonic bacteria and biofilms formed under high fluid shear conditions using a bioreactor. Results presented in this study show that AgNPs were able to inhibit the growth of an *S. mutans* clinical isolate and also kill *S. mutans* inhabiting the biofilm matrix, suggesting that AgNPs could be used for the treatment of dental caries. [3]

2. MATERIAL AND METHODS 2.1. SYNTHESIS OF AGNPS

Silver nanoparticles with spherical and pseudospherical shapes with three different sizes were synthesized. All preparations started with a 0.01 M AgNO₃ solution placed in a 250 ml reaction vessel. Under magnetic stirring, 10 ml of deionized water containing gallic acid (0.1 g for 9.3 and 78.7 nm samples and 0.5 g for 21.3 nm sample) was added to 100 ml of silver nitrate solution. After the addition of gallic acid the pH value of the solution was immediately adjusted (for the 9.5 nm sample the pH was raised to 11 with NaOH 1.0 M and for the 25.9 nm sample, pH was raised to 10 with NH₄OH). For the 78.7 nm sample, after the addition of gallic acid, the mixture was irradiated with UV light (254 nm, 15W) for 30 min (pH was not modified). After that, the solution was heated for 30 min at 80 °C. Immediately after the synthesis and in order to purify the silver nanoparticles, the obtained dispersions were dialyzed using a dialysis membrane (12 kDa molecular weight) for 48 h. [4]

2.2. Characterization Of The Agnps

AgNPs were characterized by Dynamic Light Scattering (DLS), the hydrodynamic diameter and zeta potential were determined in triplicate by using a Malvern Zetasizer Nano ZS (Instruments Worcestershire, United Kingdom) operating with a He-Ne laser at a wavelength of 633 nm, and a detection angle of 90°; all samples were analyzed for 60 s at 25 °C. To confirm shape, each sample was diluted with deionized water and 50 µl of each suspension was placed on a copper grid for Transmission Electron Microscopy (TEM). All samples were analyzed by Transmission Electron Microscopy (JEOL JEM-1230, Tokyo, Japan) at an accelerating voltage of 100 kV. [5]

2.3. Patients

The study included saliva from subjects with primary dentition, all residents of the city of San Luis Potosí, Mexico. Subjects were recruited by the department of Pediatric Dentistry of the Advanced General Dentistry Program. The children's parents completed a standardized health questionnaire that included oral pediatric information and assessments, as well as the recently used antibiotics. A voluntary informed consent was obtained from parents prior to the clinical examination, the research was done according to the Helsinki Declaration of 1975, and approved by the Masters Degree in Dental Science with Specialization in Advanced General Dentistry Program at San Luis Potosí University, Mexico. Pediatric samples of patients with active caries without any repair were considered. The inclusion criteria were children aged between 3 and 6 years. Exclusion criteria included those children who received antibiotics during the last three months preceding the survey. [6]

2.4. Sample Collection

Paraffin-stimulated whole saliva from children was sampled over a 5 min period in a sterilized propylene tube; this process was carried out consistently in the morning (9–10 am) to minimize the circadian rhythm effects, 2 h after the previous meal. Saliva samples were dispersed by sonication for 10 s and 10-fold dilutions were prepared in saline solution (0.9% NaCl), 100 µl of each dilution was spread by spiral bacteria plate (in duplicate) onto Mitis-salivarius agar (MSA) supplemented with 20% sucrose and 1% potassium tellurite. The plates were incubated in an atmosphere of 10% CO₂ at 37 °C for 24 hours (h); then plates were incubated for 24 h at room temperature. A stereoscopic microscope (Olympus, SD-ILK, Japan) was used to verify the presence of colony forming units (CFU) resembling *S. mutans*.

2.5. Bacterial Culture

Microorganism strains were maintained in solidified broth using 1.5% agar trypticase soy plate supplemented with 5% sheep blood, cultures were placed in a humidified atmosphere supplemented with 5% CO₂ for 24 h in stagnant condition. The clinical strain was identified using a VITEK® system (data not shown).

2.6. Antimicrobial Test

The micro dilution method for estimation of minimum inhibitory concentration (MIC) values was carried out to evaluate the antimicrobial activity. The MIC values were determined on 96-well micro dilution plates and according to published protocols. MICs were determined by incubating *S. mutans* in 96-well microplates in a humidified atmosphere supplemented with 5% CO₂ for 24 h. Microorganisms were exposed to serial dilutions of the nanoparticles, and the end points were determined when no turbidity in the well was observed. The antibacterial activities of the nanoparticles were compared to oxacillin. The turbidity background from the nanoparticles was subtracted from the final reading. All assays were carried out in triplicate. [7]

2.7. Biofilm Formation On Coupons

Anti-biofilm activity of the 9.5 nm AgNPs was evaluated on high shear biofilm grown in the CDC Biofilm Reactor (CDC-BR) (model CBR 90, Bio surface Technologies Corporation, Bozeman, MT) according to published protocols. Briefly, the CDC-BR consists of a 1 L vessel with eight polypropylene coupon holders, which can accommodate three sample coupons (0.5 inch diameter) in each of the eight holders. Liquid growth medium enters through the top of the vessel and exits via a side-arm discharge port. A magnetic stir bar incorporating a mixing blade provides fluid mixing and surface shear creating a turbulent flow (Reynolds number between 800 and 1850). For these calculations, the bulk fluid was assumed to possess the properties of water at 20 °C when growing a *S. mutans* biofilm. The reactor was filled with 400 ml of 1% strength TSB and inoculated with 1 ml of an overnight culture of *S. mutans*. The reactor was maintained in a batch mode (mixed, no flow) for 24 h at 37 °C. At the end of the first 24 h flow (1% strength TSB) was started and maintained for another 24 h. [8]

2.8. Microscopic Imaging Of Biofilms

After biofilm formation in the CDC-BR, coupons were removed from the reactor, rinsed with 1 ml of PBS and treated with 1 ml of different sizes of AgNPs (9.5, 25.9 and 78.7 nm) for 24 h. Each coupon was fixed in glutaraldehyde and alcian blue of analytical grade for 24 h immediately after removal. Subsequently, the coupons were dehydrated with ascending concentrations of ethanol. Completely processed

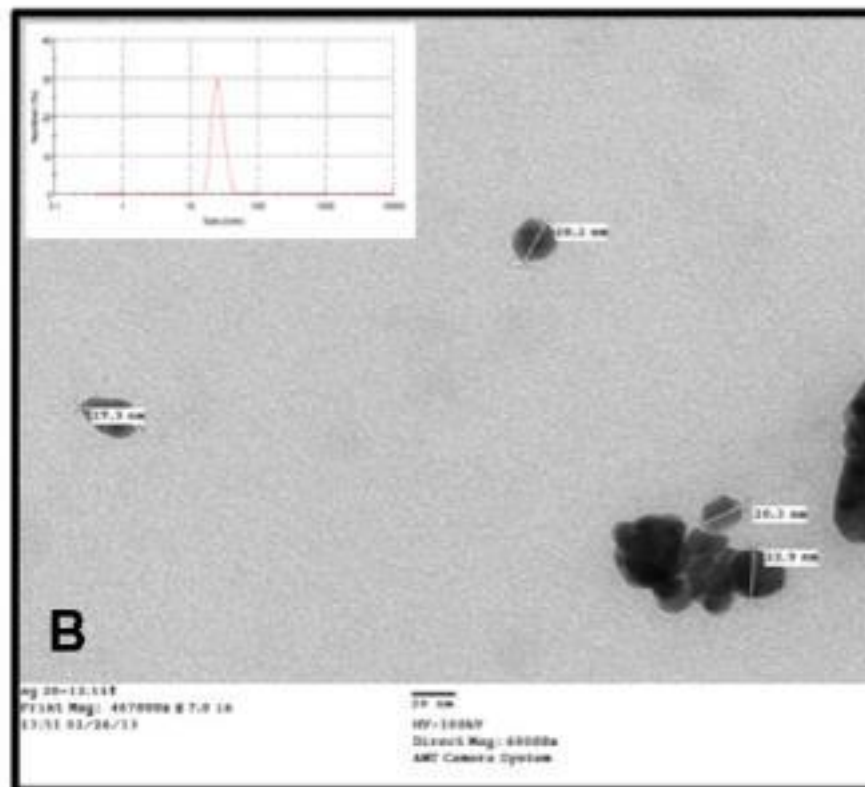
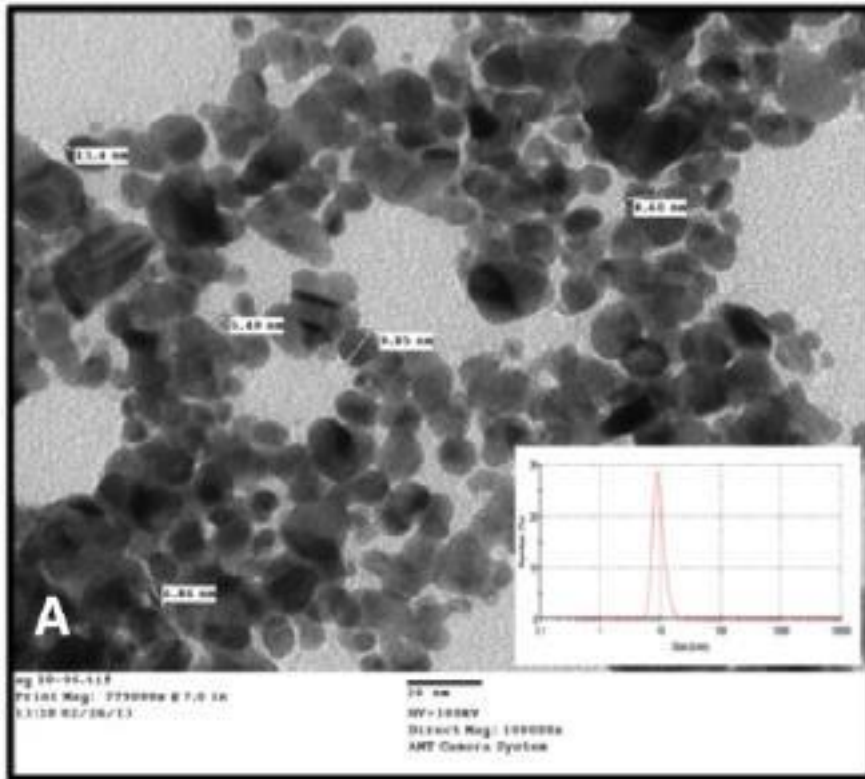
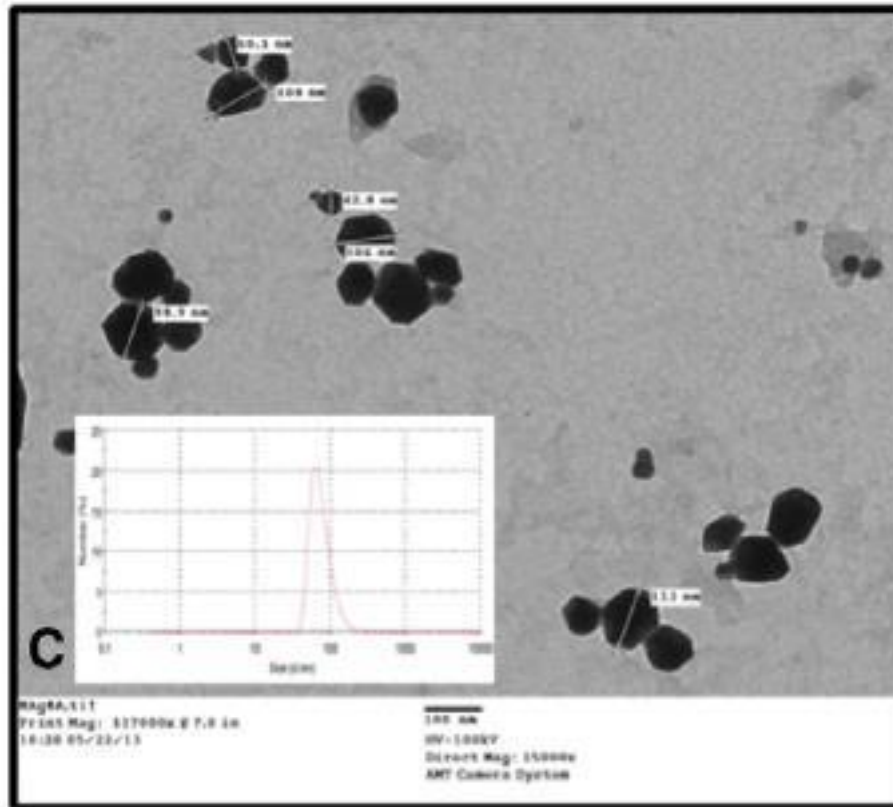


FIG: characteristics of nanoparticles used in this work. Transmission electron micrographs of silver nanoparticles at hydrodynamic size of (A) 9.5 ± 1.1 nm, (B) 25.9 ± 1.1 nm and (C) 78.7 ± 19.2 nm.

samples were mounted separately on SEM disks, coated with gold, and examined with a scanning electron microscope (JEOL 6510HV) operated at an accelerating voltage of 15 kV, the study allowed us to know the dispersion of the AgNPs over the biofilm using a Backscattered electron detector (BSE). Captured images of the external surface of each coupon at WD of 8 to 11 mm were subsequently analyzed for biofilm; images obtained at higher magnifications were assessed only for the presence of bacterial cells and typical biofilm structure. The presence of



biofilm was considered possible if a biofilm-like matrix was visible and if bacterial cell-like structures could be seen. The presence of bacterial cells was considered possible when cells consistent with cocci (0.5 to $1 \mu\text{m}$) were visible and had at least one of the following characteristics: evidence of dividing cells or cell clustering consistent with micro colony formation. [9]

2.9. Colony Counting

After biofilm formation, coupons were removed from the reactor, Rinsed with 1 ml of PBS and treated with 1 ml of different concentrations (100, 250, 500 and 1000 ppm) of AgNPs of size 9.5 ± 1.1 nm for 24 h. After the treatments, the coupons were rinsed again with 1 ml of PBS and analyzed by plate counting. Three coupons from each treatment were used to quantify the number of bacterial cells. Coupons were removed and immersed in 9 ml of sterile buffered saline solution. Biofilms were disaggregated using a sequence of treatments, which included vortexing (Vortex Genie 2; Scientific Products), sonication, and vortexing again alternating 120 second cycles of sonication at a frequency of 42 kHz (model 2510 sonicating water bath; Branson), followed by a 30 second vortexing and according to published protocols. The biofilm suspensions obtained after the treatments were serially diluted in sterile buffered saline solution, plated in triplicate on the corresponding plates, and incubated under conditions mentioned above. The CFU was counted after 18 h of incubation.

2.10. Viability Evaluation

In order to know the behavior of silver nanoparticles on human fibroblasts, a cell viability assay was performed. The consent and experimental protocols in this study were reviewed and approved by the ethics committee of Instituto Nacional de Rehabilitación (México, D.F.). Fibroblasts were obtained from circumcision surgeries from pediatric foreskin (with informed consent), the epidermis was separated from the dermis using dispase (SIGMA) for 8 h; the dermis was treated for 4 h with collagenase I (Worthington Biochemical) to obtain the fibroblasts. Cells were cultured with DMEM-F12 medium (GIBCO) supplemented with 10% BFS (GIBCO) and 1% penicillin/streptomycin (GIBCO), and maintained in an incubator at 37 °C, 83% humidity and 5% CO₂. Fibroblasts used in the assays were passage 3. Viability of human dermal fibroblast was evaluated using a Live/Dead viability/cytotoxicity kit for mammalian cells (Molecular probes, Invitrogen). Cells were seeded at a 30,000 cell/cm² density over 24 well culture dishes. Cells were exposed to 9.5 nm AgNPs at concentrations of 10, 50, 100, 150 and 200 ppm for 24 h. Cells were washed twice with a phosphate buffered saline (PBS) and incubated for 45min in Hank's balanced salt solution (HBSS; GIBCO) with 2 μM calcein AM and 2 μM ethidium homodimer (EthD-1). Calcein fluorescent signal was observed with a Fluorescein band pass filter and EthD-1 with a Texas red filter. Images were captured and analyzed using an Axiovision Observer A.1 microscope (Zeiss). [9]

2.11. Statistical Analysis

The density recorded for each coupon was log₁₀-transformed. All statistical calculations were performed on the log density values. For each test, the log densities were converted into a log reduction measure of efficacy. The log reduction is the mean log density for control coupons or membranes minus the mean log density for the corresponding treated coupons. Statistical analysis for significance was determined using a two-tailed t-test assuming unequal variances with $\alpha = 0.5$ and a P value ≤ 0.05 was considered to be significant. For cell viability analysis the cells were counted using Image J software, the percentage of live and dead cells was determined, and ANOVA and the Tukey test were performed for this assay.

93. RESULTS

3.1. Synthesis And Characterization Of The AgNPs

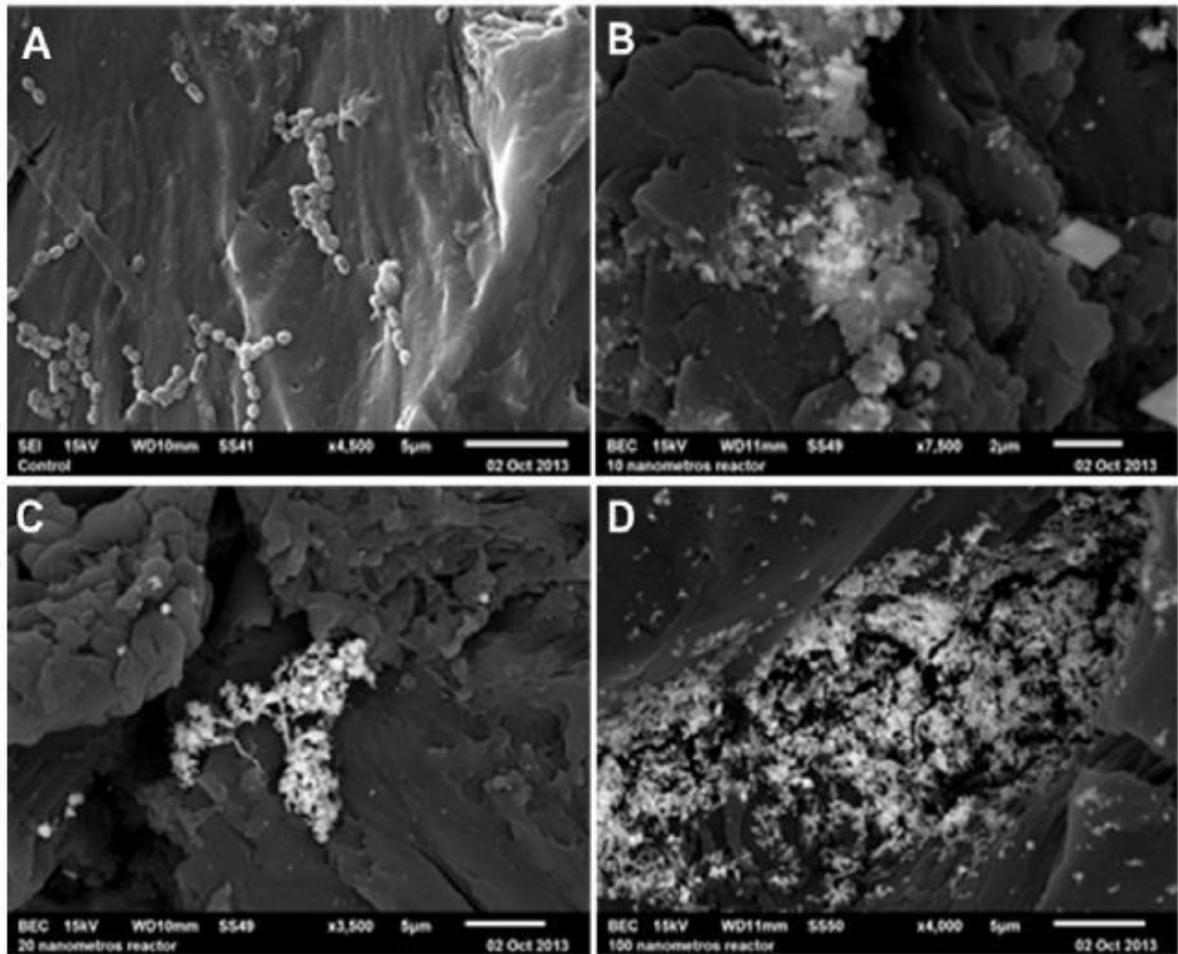
TEM revealed that AgNPs were of spherical and pseudospherical shapes. The nanoparticles synthesized in aqueous solution showed a narrow size distribution according to measures by DLS, also the hydrodynamic diameter (\pm SD) of the AgNPs was 9.5 \pm 1.1, 25.9 \pm 2.6 and 78.7 \pm 19.2 nm, and the zeta potential values range from -5.83 \pm 3.18 to -52.6 \pm 4.25 mV.

3.2. Samples And Bacterial Strains

From the samples of saliva, from pediatric patients, the microbiological analysis showed that the isolated clinical pathogenic strains commonly found were associated with a primary etiological agent in caries. Strains isolated in agar culture plate presented specific morphology characteristics, showed that *S. mutans* were the more prevalent, the biochemical identification was performed by VITEK® and the confirmation of the serotype was carried out using PCR, the results of high prevalence of *S. mutans* serotype c was in correlation with the previous results reported by Espinosa-Cristóbal et al. in saliva samples of children in our region.

3.3. Antimicrobial Test

The AgNPs showed antimicrobial activity with size and concentration behavior, like previously was reported the antimicrobial activity of AgNPs against planktonic form of different microorganisms showed better results with the smallest [10].



SEM micrographs of biofilm of *S. mutans* of 24 h on CDC coupons (A) Biofilm control, biofilm after treatment with different sizes of AgNPs (B) 9.5nm (C) 25.9nm and (D) 166.5nm

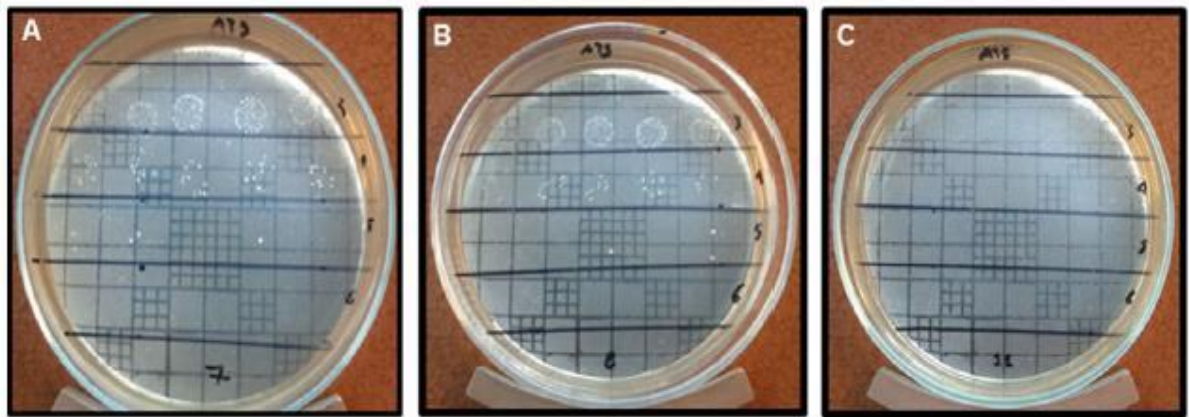
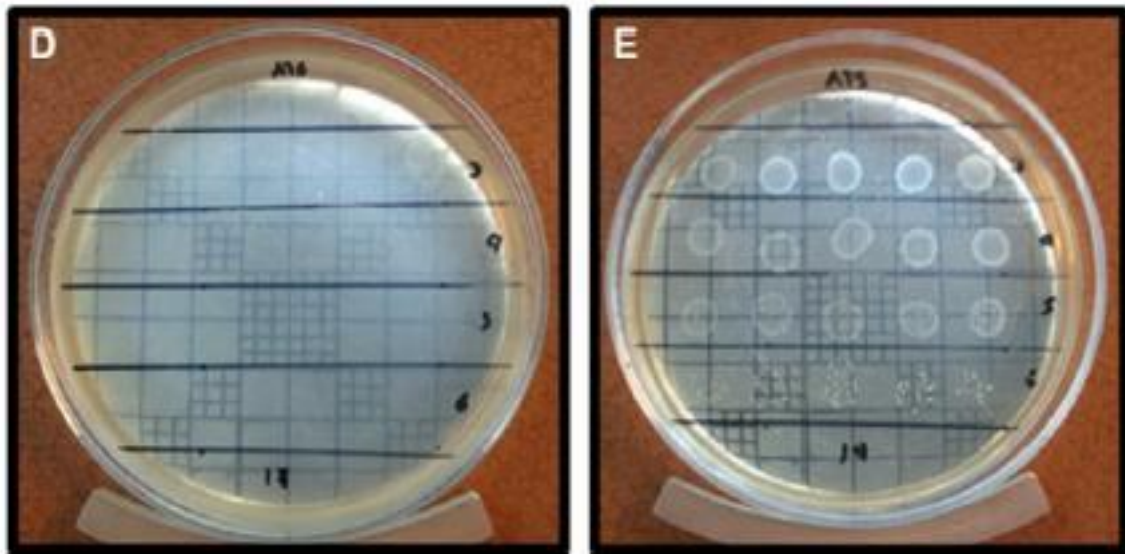


FIG: Counting the CPU assessed the survival of streptococcus mutans, for this specific experiment, after of treatment with AgNPs of 95 +/- 1.1 nm to different concentrations: (A) 100, (B) 250, (C) 500 and (D) 1000ppm, (E) control without AgNPs.

Here, the evaluation of the antimicrobial activity of AgNPs of size 9.5 + 1.1 nm against the planktonic form of clinical strain of *S. mutans* showed the highest effect, with MIC averages of 4 ± 0 ppm, which was better than that achieved with commercial antibiotic oxacillin, with an MIC average of 16 ± 0 ppm. The AgNPs with sizes 25.9 and 78.7 nm showed an MIC average of 8 and 16 ppm respectively.

3.4. Microscopic Imaging Of Biofilms

Mature *S. mutans* biofilms and individual cells were



observed with SEM, the homogeneous structure of extracellular polymeric substance (EPS) after the dehydration process was observed in the control without AgNP treatment (Fig. 2A), considering that EPS is such an integral component of the biofilm and it is a crucial target for biofilm disruption experimentation. It was possible to distinguish the contrast difference between Ag and biofilm structure due to their atomic number difference, when the Backscattered electron detector (BSE) was used. The distribution of the AgNPs of different sizes, on mature biofilm was homogeneous, and the structure of EPS was altered for the treatment with the AgNPs in comparison with the control. Fewer AgNPs were observed on the biofilm when the smallest AgNPs were used, compared to the largest AgNPs. [11]

3.5. Colony Counting

To determine the anti-biofilm activity of AgNPs, mature *S. mutans* biofilms were grown on hydroxyapatite coupons in CDC-BR. After 24 h of growth, high cell density biofilms were observed on the coupons, the coupons were treated with different concentrations (100, 250, 500 and 1000 ppm) of AgNPs of size 9.5 ± 1.1 nm, and at the same time, coupons were treated with PBS like control of growth, which showed the highest growth, all the treatments were evaluated by viable plate counts. Concentrations as low as 100 ppm of AgNPs showed a 2.3-log reduction, while increasing the AgNP concentration up to 1000 ppm resulted in a 7-log reduction. [12]

3.6. Cell Viability Analysis

For the analysis of viability we chose the AgNPs of size 9.5 ± 1.1 nm, because they showed significant activity when tested against the planktonic form, which was better than that achieved with commercial antibiotic oxacillin, as well as, the results of the biofilm structure treated with AgNPs of different sizes, AgNPs of size 9.5 ± 1.1 nm showed changes at the EPS. Viability tests with ethidium homodimer and calcein, revealed that increasing doses of silver nanoparticles killed human dermal fibroblasts as shown in the graph of cell density. AgNPs (9.5 ± 1.1 nm) were tested at concentrations of 10, 50, 100, 150 and 200 ppm in fibroblast medium. The percentages of live and dead cells were determined after 24 h of the cells being in contact with AgNPs. At a concentration of 10 ppm AgNPs did not affect fibroblast viability, but at a concentration of 50 ppm cell viability decreased by 50% and at 200 ppm most of the fibroblasts were dead, a classic dose response curve. [13]

4. DISCUSSION

Studies of NPs as antibacterial, antifouling, and antibiofilm agents have increased, and over the last few years their incorporation in new composites has been escalating. A sufficient variety of biofilm models are now commercially available or may be constructed in the laboratory.

FIG 4: Antimicrobial activities of AgNPs against biofilms formed in the CDC reactor. The mean +/- SD of three independent experiments are shown above. P value <= 0.05.

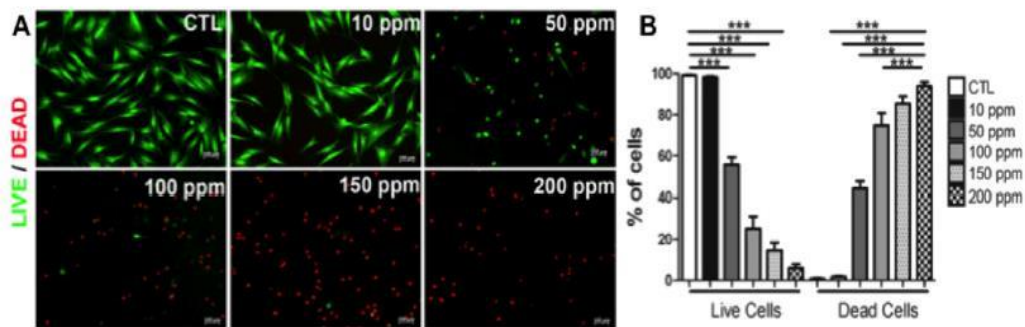
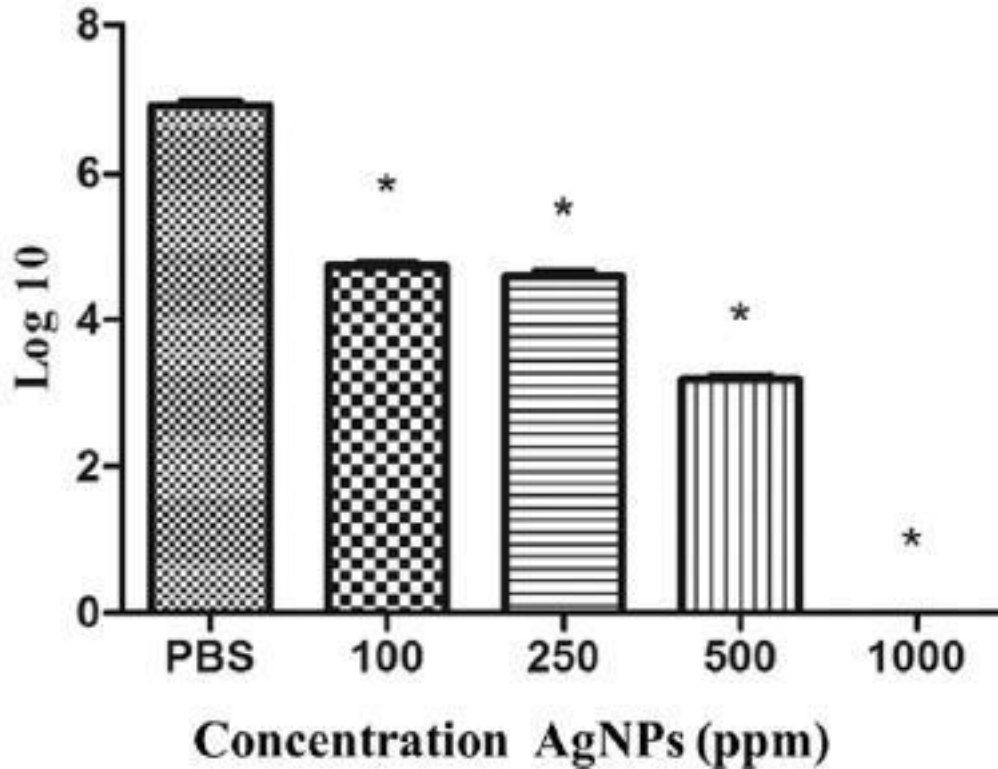


Fig. 5. Cell viability and cell death, using fibroblast for the analysis. (A) Viable cells are shown in green (calcein positive) while dead cells are in red color (ethidium homodimer positive cells). (B) Graph with response of the different concentrations.

One of the main issues for uninitiated researchers is making a rational choice regarding the best model to use. Generally, systems that closely reproduce in situ conditions should be chosen when the aim is solely to reproduce natural biofilms under laboratory conditions. The use of a CDC reactor is favored because of its standard protocol, which has been systematically evaluated. When run according to standard procedures the CDC-BR has shown to be reliable and is relatively insensitive to minor perturbations in the time allowed for initial surface colonization, culture temperature, nutrient concentration and fluid shear stress, in fact, it provides reproducible biofilm samples under consistent growth conditions for the evaluation of antimicrobial agents and surface materials. In the context of application of the nanotechnology to biological area, one study with a bonding agent containing nanoparticles of silver developing a resin–mica sandwich revealed that AgNP-containing adhesive had a long-distance killing capability and inhibited bacteria on its surface and away from its surface in a 24-well plate model . Here We report a

MIC of 4 ppm and 2.3 log reduction of *S. mutans* biofilms from 9.5 ± 1.1 nm AgNPs at concentrations ≥ 100 ppm. Care is required when interpreting data derived from this type of model, since previous research has demonstrated that biofilm grown under high fluid shear conditions, CDC-BR, produced the smallest LR and biofilm grown in the absence of fluid shear produced the largest LR. These results are in line with previous studies reporting that biofilms grown in turbulent flow conditions showed more mass resulting in an increase of the density, physiological activity, and total protein when compared to biofilms generated under static conditions. AgNPs' effect on biofilm may be due to the interference or inhibition of the bacterial machinery that controls the internal production and/or regulation of

EPS.[14] The mechanism of deactivation of proteins can be explained by the reaction of Ag⁺ ions with cysteine residues present in proteins as demonstrated in a previous study which exposed the human hepatoma HepG2 cells to N-acetyl-cysteine (NAC), an antioxidant and glutathione precursor prior to AgNP exposure. Results of this study showed that NAC treatment was equivalent to untreated controls. Then, as a result of an ionization of the AgNPs, Ag⁺ ions can interact with protein and enzyme thiol groups, such as cysteines with further damage. Results of the present study show that AgNPs kill the biofilm-associated bacteria. Further studies are needed to investigate the role of Ag⁺ ions in AgNP toxicity and diffusion through the biofilm. To examine this bactericidal activity, higher concentrations of AgNPs (ranging between 100 and 1000 times) are necessary to kill microbes within biofilms as compared to concentrations needed to kill planktonic forms. These results agree with the previous work of Ashkarran AA et al., which concluded that AgNPs should have dual toxicity effects (high toxic effect on bacteria and no/low toxic (biocompatible) effect on human cells). This investigation shows that functionalized AgNPs covering the surfaces would provide great potential for the prevention and treatment of infections related to biofilm formation. However, further research and development are necessary to translate this technology into therapeutic and preventive strategies. [15]

5. CONCLUSIONS

AgNPs effectively prevent biofilm formation and kill bacteria in established biofilms, which suggests that they could be embedded into the matrices or material used for the fabrication of medical devices to avoid adherence, colonization and biofilm formation of microorganisms. Further research and development are necessary to translate this technology into therapeutic and preventive strategies.

REFERENCES:

- [1] C.C. Goller, T. Romeo, Environmental influences on biofilm development, *Curr. Top. Microbiol. Immunol.* 322 (2008) 37–66.
- [2] T.F. Maha, G.A. O'Toole, Mechanisms of biofilm resistance to antimicrobial agents, *Trends Microbiol.* 9 (2001) 34–39.
- [3] P.S. Stewart, J.W. Costerton, Antibiotic resistance of bacteria in biofilms, *Lancet* 358 (2001) 135–138.
- [4] J.W. Costerton, Bacterial attachment to surfaces, in: D.C. Eckey (Ed.), *The Biofilm Primer*, Springer, Berlin 2007, pp. 36–43.
- [5] L.O. Bakaletz Bakaletz, Bacterial biofilms in otitis media: evidence and relevance, *Pediatr. Infect. Dis. J.* 26 (2007) S17–S19.
- [6] J.C. Post, N.L. Hiller, L. Nistico, P. Stoodley, G.D. Ehrlich, The role of biofilms in otolaryngologic infections, *Curr. Opin. Otolaryngol. Head Neck Surg.* 15 (2007) 347–351.
- [7] R.A. Brady, J.G. Leid, J.H. Calhoun, J.W. Costerton, M.E. Shirtliff, Osteomyelitis and the role of biofilms in chronic infection, *FEMS Immunol. Med. Microbiol.* 52 (2008) 13–22.
- [8] N. Høiby, Understanding bacterial biofilms in patients with cystic fibrosis: current and innovative approaches to potential therapies, *J. Cyst. Fibros.* 1 (2002) 249–254.
- [9] G.A. James, E. Swogger, R. Wolcott, E. Pulcini, P. Secor, J. Sestrich, J.W. Costerton, P.S. Stewart, Biofilms in chronic wounds, *Wound Repair Regen.* 16 (2008) 37–44.

- [10] P.E. Kolenbrander, J. London, Adhere today, here tomorrow: oral bacterial adherence, *J. Bacteriol.* 175 (11) (1993) 3247–3252.
- [11] R.A. Bagramian, F. Garcia-Godoy, A.R. Volpe, The global increase in dental caries. A pending public health crisis, *Am. J. Dent.* 22 (1) (2009) 3–8.
- [12] R.J. Palmer Jr., Composition and development of oral bacterial communities, *Periodontol.* 64 (1) (2014) 20–39 (2000).
- [13] P.E. Kolenbrander, R.J. Palmer Jr., S. Periasamy, N.S. Jakubovics, Oral multispecies biofilm development and the key role of cell–cell distance, *Nat. Rev. Microbiol.* 8 (7) (2010) 471–480.
- [14] F.E. Dewhirst, T. Chen, J. Izard, B.J. Paster, A.C. Tanner, W.H. Yu, A. Lakshmanan, W.G. Wade, The human oral microbiome, *J. Bacteriol.* 192 (2010) 5002–5017.
- [15] J.A. Lemos, R.G. Quivey Jr., H. Koo, J. Abranches, *Streptococcus mutans*: a new Grampositive paradigm? *Microbiology* 159 (Pt 3) (2013) 436–445.